

# Structural Monitoring Using GNSS Technology and Sequential Filtering

Stefano GANDOLFI, Luca POLUZZI and Luca TAVASCI, Italy

**Keywords:** GNSS, Kinematic Positioning, RTKLIB, Structural Monitoring, Garisenda Tower, Sequential Filtering

## SUMMARY

GNSS technology is still not considered as a suitable method for structural monitoring because of its relatively low precision, despite the increase in acquisition frequencies. This paper aims to evaluate a strategy for filtering a daily kinematic GNSS solution using a movement smoothing model based on the observations of previous days, so as to obtain a less scattered solution. A test was conducted with a permanent GNSS station located on top of the medieval Garisenda tower in Bologna (Italy), as it is an important part of the city's cultural heritage and a reliable test site. Because of the presence of the adjacent Asinelli tower, which is taller than the Garisenda, sky visibility is not optimal here, and for this reason a particular sequential filtering can be adopted in order to obtain more accurate solutions. The test was performed using RTKLIB software to calculate 1 Hz baselines between the test station and a master one located on a stable area about one kilometer away from the tower. In order to obtain reliable results, several variables were considered both in the data processing phase and in defining the filter. All results are reported and discussed in detail in the paper. The test results reveal a reduction in scatter of about 20% in the filtered kinematic time series, especially in weaker geodetic components.

# Structural Monitoring Using GNSS Technology and Sequential Filtering

Stefano GANDOLFI, Luca POLUZZI and Luca TAVASCI, Italy

## 1. INTRODUCTION

The monitoring of structures, land, cultural heritage and so forth has great importance today and thanks to advanced technologies, "early warning systems" have increasingly become a focus of interest (Blewitt et al., 2009). Many different sensors are available for this purpose and each one has its strengths and weaknesses. For instance, the classical topographic techniques are very precise, but they are expensive and too complicated to implement for continuous monitoring, whereas alternative topographical techniques are usually affected by time drifts and unable to detect slow movements. Integrating technologies of a different nature is always advantageous, especially if the monitored object may have either rapid or slow movements. GNSS (Global Navigation Satellite Systems) enable continuous automated monitoring of single points with relatively inexpensive instrumentation. The main weakness of GNSS compared to the other usual techniques is the lower precision of the solutions, particularly in the case of the kinematic approach needed for "near real time" applications. Nevertheless, it can provide relative positions tied to a stable reference station. As is well known, the ultimate accuracy of a GNSS solution also depends on the visibility conditions of the sky, which have to be as open as possible. When the boundary conditions are less than optimal, the final solution can be characterized by biases that are localized in particular time windows and due mainly to the constellation geometry or multipath effects (Wubben et al., 2001). With the aim of reducing these effects, many studies have investigated the possibility of modeling the effects themselves based on the solutions of previous days and have proposed methods to this end. Several authors have defined different techniques for mitigating the multipath effect from calculated coordinates (Bock et al., 2000; Forward et al., 2003, Ragheb et al., 2007). Starting from the background art, this paper proposes a method to reduce scatter in the GNSS data relying on a model generated on the basis of previous data acquired over several days. All of the results refer to a particular case study, the Garisenda Tower located in Bologna (Italy).

## 2. CASE STUDY: THE GARISENDA TOWER IN BOLOGNA



Figure 1 – The “Two Towers” of Bologna: on the left an historical representation and on the right a contemporary photo. The Garisenda tower is the shorter of the two, located on the left of each image, and the taller one (on the right) is named “Asinelli”

In this study, two weeks of data acquired by a GNSS station located on the top of the Garisenda tower of Bologna (Italy) were used. The Garisenda tower is one of the most important features of Bologna’s cultural heritage, but it is notoriously affected by problems of stability and has already been monitored using different techniques (Baraccani et. al, 2014). Moreover, the adjacent Asinelli tower constitutes an example of an unavoidable obstacle to satellite signals, which may affect GNSS solutions and have to be considered a habitual problem in these applications. As shown in Figure 1, the Asinelli tower is about 50 meters taller than the Garisenda tower and stands very close to it, on the south side. The Garisenda tower can be dated to around the last two decades of the eleventh century and during construction the foundation soil underwent subsidence phenomena (Giordano, 2000). This caused the tower, originally about 60 m tall, to tilt markedly. Today it stands at a height of 48 m and has a slope of 3.22 m towards the northeast. Therefore, several projects have been undertaken to reinforce the structure over the last decade and after completion of the work, at the beginning of the year 2011, a monitoring system<sup>1</sup> was installed on the tower in order to monitor its structural behavior by means of a long-base deformometer, deformometer, extensimeter, laser displacement sensor and inclinometers. In 2013, the Department of Civil, Environmental and Materials Engineering of Bologna University installed a permanent GNSS station on the roof of the Garisenda for the double purpose of monitoring the building and testing the satellite technology for this type of application. The station acquires 1 Hz GNSS data and send them via mobile phone technology to a computer server that stores all the received raw data.

---

<sup>1</sup> [http://www.tecnoinmonitoraggi.it/cms\\_descrizione\\_sistema\\_monitoraggio.html](http://www.tecnoinmonitoraggi.it/cms_descrizione_sistema_monitoraggio.html)

### 3. DATA PROCESSING

The GNSS data were processed using the free RTKLIB software package (Takasu et al. 2007), which features several calculation modes (Takasu, 2009). Kinematic differential post processing was used to calculate baselines between the Garisenda station (BOGA) and a reference one (BOL1) located on the roof of the School of Engineering and Architecture of Bologna University, about 1.6 km away from the tower.



Figure 2 – Map of BOGA and BOL1 location

Both stations provide 1 Hz data. For this study, 15 days of data were processed; these days were chosen because of the good continuity in the data stream, which is often affected by a lack of GSM signals.

Despite the short length of the baseline between the GNSS stations, some parameters may have an impact on the data processing, the carrier phase (or a combination of different carrier phases) and the cut-off angle in particular.

With regard to the carrier phase, a test was performed to compare the L1 solution with L1+L2. Because of the short baseline length, other combinations were not considered. This test showed that the use of only one frequency (L1) makes it possible to have a higher number of fixed solutions (+10%), but at the same time results in a higher RMS (+22% on average). Thus it was decided to use the carrier frequencies L1 + L2.

The elevation mask is a parameter that, in particular boundary conditions, can significantly affect both the accuracy and scattering of solutions. In particular, when obstacles are present, they limit sky visibility and produce multipath effects. Figure 3 shows the cycle slip map area located in the southern part of the skyplot and the multipath graph, which reveals a high correlation between multipath effects and SNR quality.

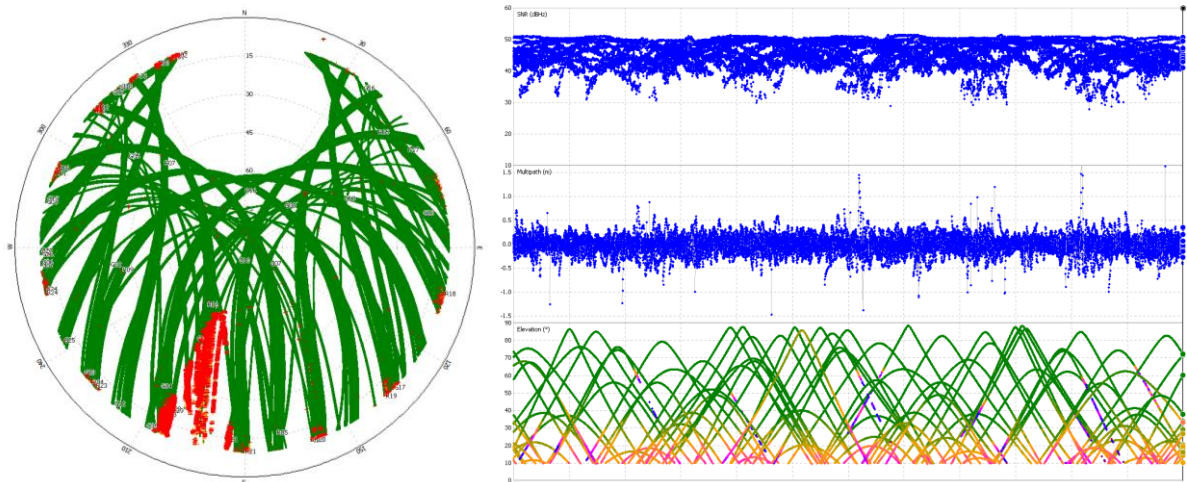


Figure 3 – Cycle slip skyplot (left) and SNR/Multipath/Elevation graphs (right) of BOGA site (DOY: 355 year: 2013).

In light of these considerations, as a preliminary test, four different calculations were performed using different elevation masks ( $10^\circ, 13^\circ, 15^\circ, 25^\circ$ ). The test was performed on the whole dataset and has evidenced how the best results, in terms of scattering of the solutions, were obtained for a  $10^\circ$  elevation mask (Table 1).

Elevation mask	$\sigma_N$ (mm)	$\sigma_E$ (mm)	$\sigma_U$ (mm)
$10^\circ$	5.7	4.1	8.9
$13^\circ$	6.4	8.0	9.4
$15^\circ$	7.2	6.4	13.0
$25^\circ$	120.7	59.9	199.9

Table 1 - Repeatability of the kinematic solution in terms of standard deviation considering different elevation mask angles for data processing.

The main calculation parameters adopted for the data processing are listed below.

- Constellation: GPS+GLONASS
- Observables: Carrier Phase
- Frequencies: L1+L2
- Position Mode: kinematic
- Filter Type: Forward
- Ionosphere Correction: Broadcast
- Tropospheric Correction: Saastamoinen
- Satellite Ephemeris/Clock: IGS Precise
- Data sampling: 1Hz

All calculations, results and graphs have been represented in a geodetic local reference frame where the origin was defined using 15 days of static data processing. The reason for this choice was the need to separate the plane components from the height one.

The first results revealed a higher scattering of solutions for the North component compared to the East one, which is quite unusual for the GNSS technique, but could be explained by considering the

obstacle in the southern sky represented by the Asinelli tower. The time series of the three geodetic components shown in Figure 4 provide evidence of some recursive systematic effects. It is unlikely that they represent the movement of the structure. We investigated the solutions in detail and evaluated the possibility that the difficulties in estimating the coordinates could be due to the satellite constellation.

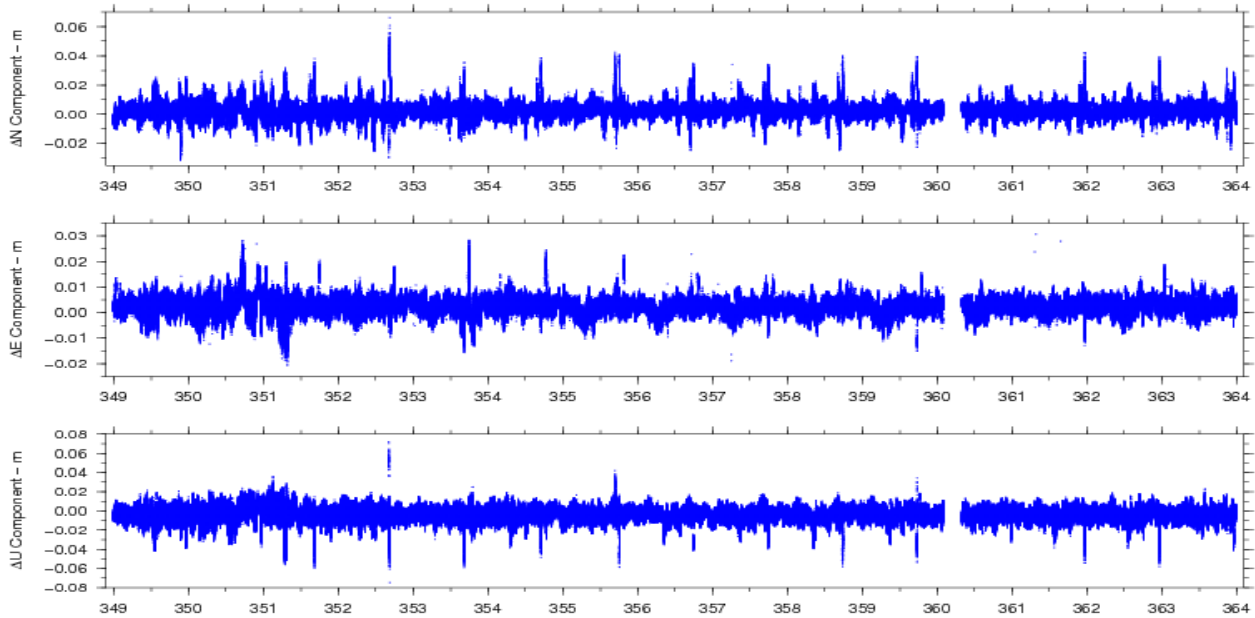


Figure 4 – Kinematic time series of 15 days in the Local Geodetic components (N,E,U), cleaned of outliers. The X-axis is expressed in DOY of the year 2013.

In particular, the presence of some regular spikes over the complete time series was examined in depth. The autocorrelation function (Cliff and Ord, 1973) was applied to the solutions; the results obtained are shown in Figure 5. The highest peak was located at 86164 seconds, which represents the sidereal day (Radovanovic, 2000), indicating the recursive GNSS constellations. As the systematic effects are constant, it is conceivable to create a daily empirical model with the aim of smoothing the original solution and obtaining more stable results. Below we describe the strategies adopted to create the daily models and the results obtained for the dataset considered.

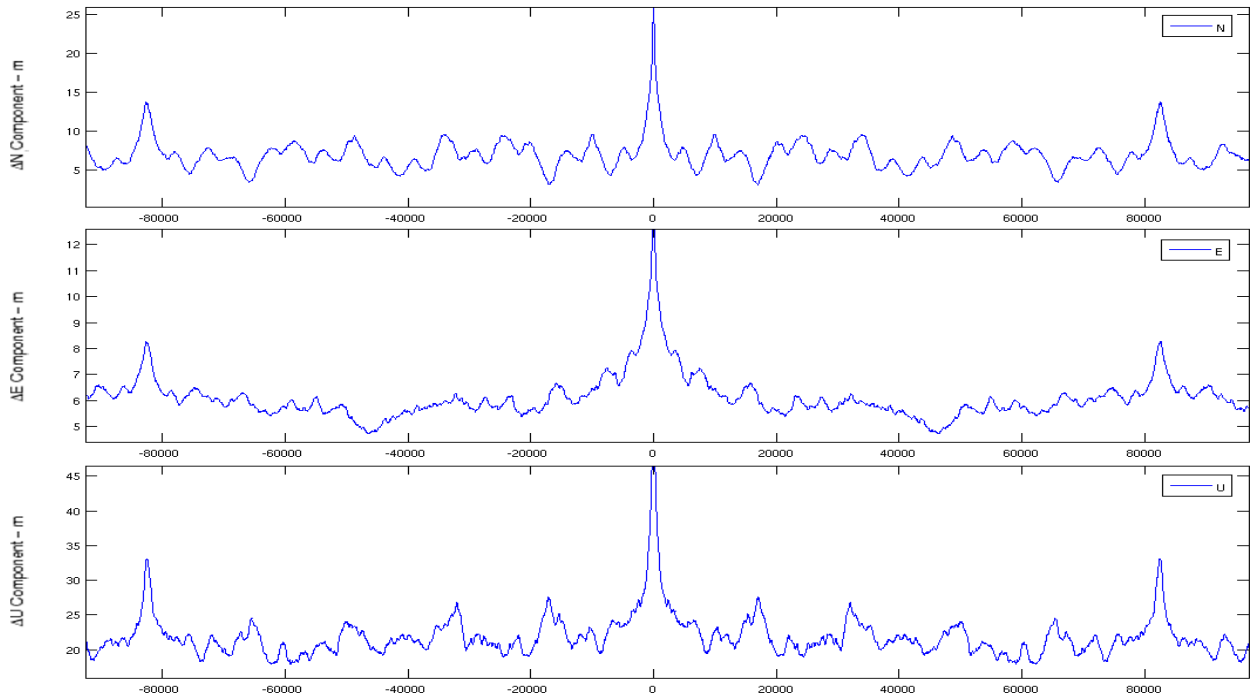


Figure 5 – Autocorrelation function in the three Local Geodetic components (N,E,U). The x-axis is represents the time delay expressed in seconds.

#### 4. DEFINITION OF THE SMOOTHING MODEL

The results obtained using the autocorrelation function provide evidence of a recursive effect with the amplitude of a sidereal day. This effect is not due to movements of the structure and can be reduced by creating a model from the solution of previous days. The model has to have the length of a sidereal day.

In order to create such a model, several steps have to be performed. The first step consists in the rejection of outliers. This was achieved by means of an iterative process based on the hypothesis of linear motion of the solution for very short time windows. The main reason for splitting the time series into short blocks is to preserve the predominant pattern of the time series and remove just single spikes or outliers. For this purpose, every day was divided into 30 periods of 2880 seconds each and then a linear regression for each component was computed using a traditional weighted least squares approach. The weight assumed for the computation was the inverse of the formal variance derived from the data processing. With  $i$  defined as the component (North, East and Up), the slope  $m^i$  and the y-axis intercept  $q^i$  of the linear regression were obtained for each period, thus enabling a calculation of the residuals  $v^i(t)$ :

$$v^i(t) = S^i(t) - [q^i + m^i * t] \quad (1)$$

where  $S^i(t)$  represents the solution of the  $i$ -th component at the epoch  $t$ .

An iterative loop was used to seek and remove the furthest outlier by comparison of the maximum residuals with the standard deviation  $\sigma$ , calculated as:

$$\sigma^i = \sqrt{\frac{\sum_n v^i(t)^2}{n}} \quad (2)$$

where  $n$  is the number of solutions for each block ( $\max\{n\}=2880$ ). We assumed a solution to be an outlier when one of the three associated residuals was more than 3 times larger than the associated standard deviations. If a solution was considered as an outlier, it was removed from the time series and all the sequences resulting from the calculation of the linear regression and rejection of outliers were re-processed.

The time series without outliers ( $C^i(t)$ ) were subsequently used to generate the sidereal filter. From the cleaned daily time series we generated files containing *sidereal daily* time series (with a length of one sidereal day – 86164 seconds). From these files a sidereal daily model was calculated by means of a weighted running average of  $2r + 1$  seconds (for the first and last  $r$  epochs of each sidereal day; data were taken from the previous or subsequent sidereal days).

For each block of  $2r+1$  data, the average value was calculated using the following equation:

$$d^i(t^*) = \sum_{\tau=i-r}^{i+r} \frac{C^i(\tau)}{(\sigma^i(\tau))^2} / \sum_{\tau=i-r}^{i+r} \frac{1}{(\sigma^i(\tau))^2} \quad (4)$$

with

$$t^* = \frac{\sum_{\tau=i-r}^{i+r} \tau}{2r+1} \quad (5)$$

Where  $\sigma^i(\tau)$  represents the formal error associated with the  $C^i(\tau)$  solution,  $d^i(t^*)$  represents the value of the model for the  $i$ -th at time  $t^*$  and  $t^*$  represents the mean time of the values considered. The reason for this definition, as regards both the model and associated time, is to compensate for any possible lack of data. Where data are lacking, the value of the running average has to be located at the mean time relative to the considered data. The model created was not equally spaced in time and in order to remedy this aspect, the last step was to resample the model, thereby generating the final model of 86164 values (sidereal seconds).

We assumed  $m^{ik}$  as the final resampled model for the  $k$ -th day and  $i$ -th component. It is important to underline that when this method is used, the sidereal models are always full of data and a model can be estimated for each sidereal day. The smoothing model for the kinematic solution of the generic  $k$ -th day could be built using an average of several ( $d$ ) models based on previous days. We defined this smoothing model  $M^{ikd}$  as:

$$M^{ikd} = \frac{m^{i(k-1)} + \dots + m^{i(k-d)}}{d} \quad (5)$$

And the filtered solution was calculated as:

$$F^{ikd}(t) = C^{ik}(t) - M^{ikd}(t) \quad (6)$$

Considering the absence of movements during the test campaign, the standard deviation of the time series  $C^{ik}$  and  $F^{ikd}$  were taken into account to evaluate the repeatability of the solutions.

The next section is dedicated to evaluating the improvement achieved by changing the dimension of  $d$ , considering a reasonable value of the parameter  $r$ .

## 5. TEST RESULTS OBTAINED FROM THE GARISENDA TOWER GNSS STATION: RESULTS AND DISCUSSION

The value  $r$  of the seconds to be used for the moving average was first determined by carrying out several tests. Considering that an excessively high value of  $r$  does not enable rapid movements to be picked up, but on the other hand an  $r$  value that is too low does not remove the white noise, we chose  $r = 100$  seconds for all the tests.

Particular attention was given when selecting the value of  $d$ . We assessed the improvement in terms of scatter of the solutions by considering models that were generated varying  $d$  from 1 to 7 days and testing them for eight days following the seventh.

$K$	$d$	$\Delta N$		$\Delta E$		$\Delta U$	
		$\sigma^C$ (mm)	$\sigma^F$ (mm)	$\sigma^C$ (mm)	$\sigma^F$ (mm)	$\sigma^C$ (mm)	$\sigma^F$ (mm)
8	1	4.5	3.6	2.6	2.5	6.7	5.3
	2		3.6		2.3		5.2
	3		3.5		2.2		5.0
	4		3.4		2.2		4.8
	5		3.3		2.2		4.8
	6		3.3		2.2		4.8
	7		3.3		2.2		4.8
9	1	4.2	3.5	2.4	2.6	5.8	5.7
	2		3.1		2.1		5.0
	3		3.2		2.0		4.7
	4		3.1		2.0		4.6
	5		3.1		2.0		4.6
	6		3.0		1.9		4.5
	7		3.0		2.0		4.5
10	1	4.6	3.9	2.7	2.7	6.9	6.4
	2		3.7		2.6		5.9
	3		3.6		2.5		5.8
	4		3.5		2.4		5.8
	5		3.5		2.4		5.7
	6		3.5		2.4		5.7
	7		3.5		2.4		5.7
11	1	5.5	5.7	4.8	4.9	8.6	9.5
	2		5.4		4.6		8.4
	3		5.3		4.4		8.2
	4		5.2		4.4		8.0
	5		5.2		4.4		8.0
	6		5.2		4.4		8.0
	7		5.2		4.4		8.0
12	1	6.1	6.9	4.1	5.9	9.8	11.2
	2		5.6		4.5		9.0
	3		5.3		4.2		8.5
	4		5.0		4.1		8.3
	5		5.0		4.0		8.2
	6		4.9		4.0		8.1
	7		4.9		3.9		8.0
13	1	6.1	5.5	2.7	3.5	7.3	8.2
	2		5.4		3.5		7.4
	3		4.9		2.8		6.7
	4		4.8		2.6		6.3
	5		4.7		2.5		6.3
	6		4.6		2.4		6.2
	7		4.6		2.4		6.1
14	1		4.7		2.5		5.5

	2		4.1		2.6		5.3
	3		3.8		2.8		5.1
	4	4.2	3.6	2.7	2.6	5.7	4.8
	5		3.5		2.4		4.7
	6		3.5		2.4		4.7
	7		3.4		2.4		4.7
15	1		4.0		3.3		6.4
	2		3.7		3.0		6.2
	3		3.6		3.2		6.3
	4	4.4	3.6	3.2	3.1	7.0	6.0
	5		3.5		3.0		6.0
	6		3.4		2.9		5.9
	7		3.4		2.9		5.8

Table 2 – Standard deviation of the daily kinematic solution filtered by models calculated using an increasing number of preceding days ( $d$ ). Column 1 shows the day of the filtered solution; column 2 shows the value of  $d$ ; columns 3, 5 and 7 show the standard deviation of the original cleaned solution for components N, E and U, respectively, whereas columns 4,6 and 8 show the standard deviation of the filtered solutions.

The results in terms of scattering and the improvements obtained with the  $F^k$  time series compared to the  $C^k$  time series are shown in Table 2 and Table 3, respectively.

Scatter reduction		$D$						
Component	$K$	1	2	3	4	5	6	7
$\Delta N$	8	19%	20%	22%	25%	27%	27%	27%
	9	16%	26%	24%	25%	27%	28%	28%
	10	16%	19%	22%	23%	23%	25%	24%
	11	-4%	2%	3%	5%	7%	6%	6%
	12	-13%	9%	14%	17%	18%	19%	19%
	13	9%	11%	19%	21%	23%	23%	24%
	14	-12%	1%	9%	13%	15%	16%	18%
	15	9%	16%	17%	18%	20%	22%	23%
	Average	7.2%	15.0%	17.9%	19.7%	20.0%	21.4%	21.1%
$\Delta E$	8	4%	12%	14%	17%	17%	17%	16%
	9	-7%	12%	18%	16%	18%	18%	18%
	10	0%	3%	8%	9%	11%	11%	10%
	11	-2%	4%	8%	9%	9%	8%	8%
	12	-44%	-9%	-2%	1%	2%	3%	6%
	13	-32%	-29%	-6%	4%	5%	8%	10%
	14	8%	7%	-2%	7%	12%	13%	14%
	15	-4%	6%	0%	3%	6%	8%	7%
	Average	-6.1%	3.7%	8.2%	11.2%	11.1%	10.9%	11.2%
$\Delta U$	8	21%	22%	26%	29%	29%	29%	28%
	9	3%	15%	20%	22%	21%	22%	22%
	10	7%	13%	16%	16%	16%	17%	17%
	11	-10%	2%	5%	7%	7%	7%	7%
	12	-14%	8%	13%	15%	16%	17%	17%
	13	-12%	-1%	9%	14%	15%	16%	17%
	14	3%	7%	12%	16%	18%	19%	19%
	15	9%	11%	10%	13%	14%	15%	16%
	Average	2.4%	11.4%	15.7%	17.6%	17.7%	19.0%	17.9%
Overall average		-1.3%	7.7%	11.6%	14.4%	16.3%	17.1%	16.7%

Table 3 – Reduction in the standard deviation of the daily kinematic solutions filtered by models calculated using an increasing number of preceding days ( $d$ ) compared to the original cleaned solution.

It may be observed from Table 2 that North is the least precise planimetric component, though the East component is usually the weaker one in GNSS. This is probably due to the specific location of the station, as the Asinelli tower is south of the Garisenda tower and thus occludes the sky in the direction that mainly influences the North determination. As shown in Table 3, the highest scatter reduction was achieved precisely in the North component, and especially where  $d=6$ . Also considering the overall improvement,  $d=6$  appears to be the best choice for this context.

Figure 6 shows an example of how the filter works over a time span of about one hour. In the figure the original cleaned solution  $C^k$  is represented by green dots, the 6-day  $M^k$  model by a blue line and the filtered  $F^k$  solution by red dots. As is evident, the filter reduces the original systematic effect, rapidly correcting the solution and bringing the values close to zero.

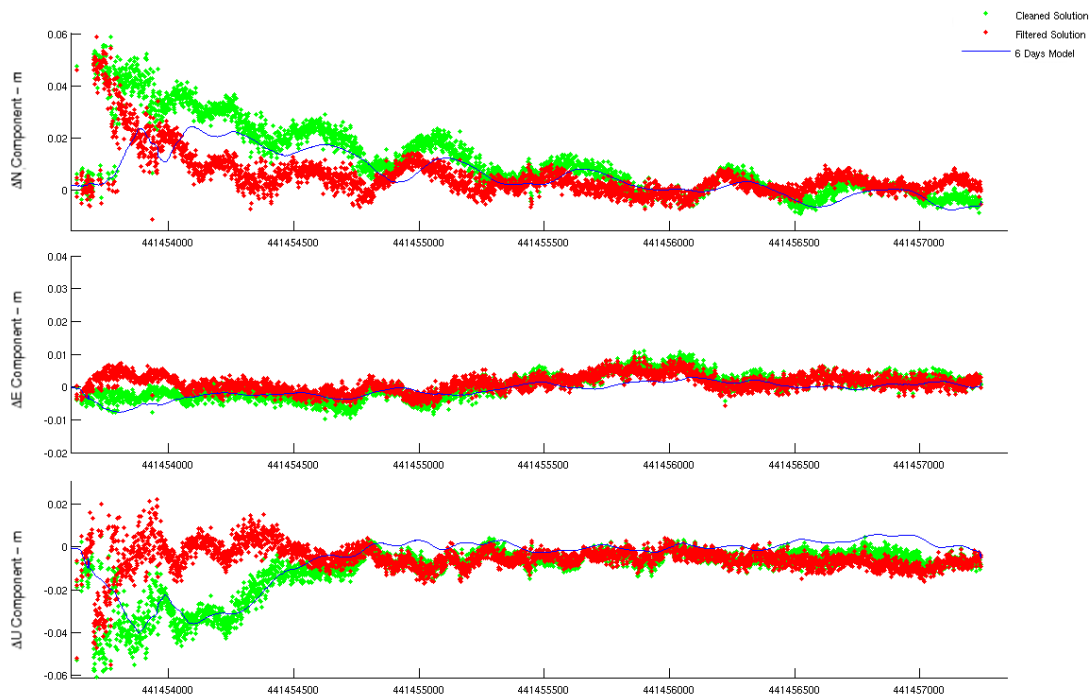


Figure 6 – Comparison between the Cleaned Solution (green), Filtered Solution (red) and 6-Day Model Applied (blue)

Finally, Table 4 provides a summary of the most significant results obtained starting from the seventh day, demonstrating the improvement of the final solution when a sequential filtering based on  $d=6$  is applied.

$k$	$\Delta N$			$\Delta E$			$\Delta U$		
	$\sigma^C$ (mm)	$\sigma^F$ (mm)	Scatter reduction	$\sigma^C$ (mm)	$\sigma^F$ (mm)	Scatter reduction	$\sigma^C$ (mm)	$\sigma^F$ (mm)	Scatter reduction
7	3.8	2.8	26%	2.2	2.0	12%	6.2	4.4	30%
8	4.5	3.3	27%	2.6	2.2	17%	6.7	4.8	29%
9	4.2	3.0	28%	2.4	1.9	18%	5.8	4.5	22%
10	4.6	3.5	25%	2.7	2.4	11%	6.9	5.7	17%
11	5.5	5.2	6%	4.8	4.4	8%	8.6	8.0	7%
12	6.1	4.9	19%	4.1	4.0	3%	9.8	8.1	17%
13	6.1	4.6	23%	2.7	2.4	8%	7.3	6.2	16%
14	4.2	3.5	16%	2.7	2.4	13%	5.7	4.7	19%
15	4.4	3.4	22%	3.2	2.9	8%	7.0	5.9	15%
Average	4.8	3.8	20.9%	3.0	2.7	10.1%	7.1	5.8	18.4%

Table 4 – Summary of the results obtained starting from the seventh day, expressed both in terms of standard deviation and percentage of improvement.

## 6. CONCLUSIONS

Boundary conditions are known to influence the quality of a GNSS solution. In particular, multipath effects or reduced sky visibility can generate daily biases in the kinematic solutions. In this paper we evaluated a strategy for improving the repeatability of a GNSS solution for monitoring purposes. The strategy is based on subtracting an empirical model from the kinematic solution. The model can be estimated on the basis of the 6 preceding daily solutions. In order to evaluate the improvements achieved by this approach, a test was performed using a GNSS receiver located on top of the Garisenda tower in Bologna, which is overlooked by the adjacent Asinelli tower. The results obtained show that it is possible to improve the solutions by about 20% in terms of scatter. The standard deviations of the residual time series were 3.8, 2.7, 5.8 mm in the North, East and Up components, respectively, as opposed to 4.8, 3.1, 7.1 mm when the data were unfiltered. This improvement serves to increase the sensitivity of the monitoring system in defining a minimum threshold of significant movement, thus enhancing its accuracy. The proposed method can be easily implemented also for real-time solutions, useful in early warning systems. Some final points warrant mention. The suggested approach can improve the solution above all in the presence of non-optimal boundary conditions. The number of days used to generate the models and the number of epochs considered in the running average should be determined on a case-by-case basis.

## REFERENCES

- Baraccani, S., Gasparini, G., Palermo, M., Silvestri, S., Trombetti, T., (2014). A Possible Interpretation of Data acquired from Monitoring Systems, Proceedings of the Twelfth International Conference on Computational Structures Technology, B.H.V. Topping and P., Civil-Comp Press, Stirlingshire, Scotland
- Blewitt, G., Hammond, W. C. Kreemer, C., Plag, H.-P., Stein, S., Okal, E., (2009). GPS for real-time earthquake source determination and tsunami warning systems. *J. Geodes.* 83, 335–343, doi 10.1007/s00190-008-0262-5.
- Bock, Y., Nikolaidis, R.M., de Jonge, P. and Bevis, M. (2000). Instantaneous Geodetic Positioning at Medium Distances with the Global Positioning System, *Journal of Geophysical Research*, Vol. 105, No. B12, pp. 28223-28255.
- A.D. Cliff, J.K. Ord. Spatial autocorrelation. Vol. 5. London: Pion, 1973.
- Forward, T., Stewart, M., & Tsakiri, M. (2003). GPS data stacking for small scale GPSdeformation monitoring applications. In Proc 11th FIGInt Symp on Deformation Measurements (pp. 233-240). Santorini: [s. n.].F. Giordano, La torre Garisenda, Fondazione del Monte di Bologna e Ravenna, Costa Editore, 2000
- Radovanovic, R. S. (2000). High accuracy deformation monitoring via multipath mitigation by day-to-day correlation analysis. In 13th International Technical Meeting of the SAT Division of the ION, September (pp. 19-22).
- Ragheb, A. E., Clarke, P. J., & Edwards, S. J. (2007). GPS sidereal filtering: coordinate-and carrier-phase-level strategies. *Journal of Geodesy*, 81(5), 325-335.
- T.Takasu, N.Kubo, A.Yasuda, (2007). Evaluation and Application of RTKLIB: A program library for RTK-GPS, GPS/GNSS Symposium 2007, Tokyo, Japan, November 20-22, 2007
- T.Takasu, (2009). RTKLIB: Open Source Program Package for RTK-GPS, FOSS4G 2009 Tokyo, Japan, November 2, 2009
- Wübbena, G., Bagge, A., Boettcher, G., Schmitz, M., & Andree, P. (2001). Permanent object monitoring with GPS with 1-millimeter accuracy. In International Technical Meeting ION GPS-01, Salt Lake City USA.

## CONTACTS

Prof. Stefano Gandolfi  
DICAM – University of Bologna  
Viale Risorgimento, 2  
Bologna, Italy  
Office: +39 0512093102  
Fax: +39 0512093114  
Web Site: